

# Modeling peculiar velocities of dark matter halos<sup>\*</sup>

Takashi Hamana<sup>1,2</sup>, Issha Kayo<sup>3</sup>, Naoki Yoshida<sup>2,4</sup>, Yasushi Suto<sup>3,5</sup> and Y.P. Jing<sup>6</sup>

<sup>1</sup> Institut d’Astrophysique de Paris, 98bis Boulevard Arago, F 75014 Paris, France

<sup>2</sup> National Astronomical Observatory of Japan, Mitaka, Tokyo 181-8588, Japan

<sup>3</sup> Department of Physics, University of Tokyo, Tokyo 113-0033, Japan

<sup>4</sup> Harvard-Smithsonian Center for Astrophysics, 60 Garden Street, Cambridge, MA 02138, USA

<sup>5</sup> Research Center for the Early Universe (RESCEU), School of Science, University of Tokyo, Tokyo 113-0033, Japan

<sup>6</sup> Shanghai Astronomical Observatory, the Partner Group of MPI für Astrophysik, Nandan Road 80, Shanghai 200030, China

arXiv:astro-ph/0305187v3 6 Dec 2004

Accepted 2003 May 5, Received 2003 April 16; in original form 2003 January 9

## ABSTRACT

We present a simple model that accurately describes various statistical properties of peculiar velocities of dark matter halos. We pay particular attention to the following two effects. First, the evolution of the halo peculiar velocity depends on the local matter density, instead of the global density. Secondly, dark matter halos are biased tracers of the underlying mass distribution, thus halos tend to be located preferentially at high density regions. For the former, we develop an empirical model calibrated with *N*-body simulations, while for the latter, we use a conventional halo bias model based on the extended Press-Schechter model combined with an empirical log-normal probability distribution function of the mass density distribution. We find that, compared with linear theory, the present model significantly improves the accuracy of predictions of statistical properties of the halo peculiar velocity field including the velocity dispersion, the probability distribution function, and the pairwise velocity dispersion at large separations. Thus, our model predictions may be useful in analyzing future observations of the peculiar velocities of galaxy clusters.

**Key words:** galaxies: clusters: general – cosmology: theory – dark matter – large-scale structure of universe

## 1 INTRODUCTION

In the standard structure formation scenario, dark matter halos are thought to be formed via the gravitational amplification of initial small density fluctuations, and their motion results from gravitational forces acting over large scales. As a consequence, the root-mean-square (rms) peculiar velocities of halos at the present time depend on the total amount of matter in the universe,  $\Omega_0$ , and on the normalization of the matter power spectrum,  $\sigma_8$ , as  $\propto \sigma_8 \Omega_0^{0.6}$ . In addition, linear theory predicts that the halo peculiar velocity evolves as  $\propto a(t) dD(t)/dt$  where  $a(t)$  is the scale factor normalized unity at the present time and  $D(t)$  is the linear growth rate (see Section 2). Thus, a measurement of the rms peculiar velocities of halos can be used as a test of structure formation scenarios in principle.

A measurement of the peculiar velocity of a dark mat-

ter halo is possible through its baryon contents. Because a cluster of galaxies is formed in the gravitational potential of a massive dark matter halo, its peculiar motion traces that of the hosting halo. Therefore, the rms peculiar velocity of clusters of galaxies provides a reasonable measure of that of halos. So far, empirical distance indicators such as the Tully–Fisher and the  $D_n$ – $\sigma$  relations have been used to measure the peculiar velocity of relatively nearby systems (e.g. Bahcall, Gramann & Cen 1994; Lauer & Postman 1994; Bahcall & Oh 1996; Moscardini et al. 1996; Borgani et al. 1997, 2000; Watkins 1997; Dale et al. 1999; Hudson et al. 1999; Colless et al. 2001). Future observations of the kinematic Sunyaev–Zel’dovich effect will provide measurements of line-of-sight peculiar velocity for distant systems (Sunyaev & Zel’dovich 1980; Rephaeli & Lahav 1991; Haehnelt & Tegmark 1996; Kashlinsky & Atrio-Barandela 2000; Aghanim, Górska & Puget 2001).

Theoretical predictions of the rms peculiar velocity of halos have been made by applying the peak theory (Bardeen et al. 1986), in which halo motions are modeled by motions of density peaks of a suitably smoothed version of the initial Gaussian density field evolved according to linear theory (Peebles 1980). *N*-body simulations have been used to test

<sup>\*</sup> This paper was published in Mon. Not. R. Astron. Soc. **343**, 1312–1318 (2003). Owing to an error in numerical computations, some incorrect results were presented there. Erratum is to be published in Mon. Not. R. Astron. Soc. Conclusions of the original version are unaffected by the correction. This version supersedes the original version.

those predictions (e.g. Bahcall, Gramann, Cen 1994; Croft & Efstathiou 1994; Suhonenko & Gramann 1999, Colberg et al. 2000; Sheth & Diaferio 2001; Yoshida, Sheth & Diaferio 2001). Colberg et al. (2000) found that, at  $z > 4$ , the mean peculiar velocities of materials that end up in massive halos agree well with the predictions of linear theory for the corresponding peaks, but that linear theory systematically underestimates their subsequent growth; the rms peculiar velocities at  $z = 0$  evaluated from  $N$ -body simulations are larger than the linear theory prediction by up to 40 percent. This discrepancy may be ascribed to the following facts: that evolution of peculiar velocities of halos in high density regions are accelerated relative to the average (Tormen & Bertshinger 1996; Cole 1997; Kepner, Summers & Strauss 1997) and that halos tend to be formed in such higher-density regions because of the biased structure formation mechanism. Sheth & Diaferio (2001) have shown using  $N$ -body simulations that the evolution of the halo peculiar velocity indeed depends on the local matter density, rather than on the global density. They presented a simple model for the shape of the distribution function of the peculiar velocities that takes into account their dependence on the local density in an empirical manner.

The purpose of this paper is to present a simple and accurate model for the rms of peculiar velocities of halos. Hereafter, we denote the rms peculiar velocity of halos with mass  $M$  as  $\sigma_{\text{halo}}(M)$ .

The major improvements that we achieve here are to take into account the following two points that play an important role in understanding statistical properties of halo peculiar velocities. (i) The evolution of the halo peculiar velocity depends on the local matter density, rather than on the global density. We develop a model of the local density-dependent growth of the halo peculiar velocity in an empirical manner following Sheth & Diaferio (2001). (ii) Dark matter halos are biased tracers of the dark matter distribution, and thus halos tend to be located at high-density regions. In order to implement this, we use the halo biasing model developed by Mo & White (1986) and Sheth & Tormen (1999; 2002) combined with an empirical log-normal probability distribution function (PDF) of the mass density distribution (Kayo, Taruya & Suto; 2001).

The outline of this paper is as follows. In Section 2, we summarize linear theory predictions for the peculiar velocities of peaks. In Section 3, we describe  $N$ -body simulations that are used to calibrate and to test the model. We construct the model in Section 4. The model predictions are compared with  $N$ -body simulations in section 5. A summary and discussion are presented in Section 6.

## 2 LINEAR PREDICTIONS FOR THE PECULIAR VELOCITIES OF PEAKS

In this section, we summarize basic equations of the linear theory predictions for peculiar velocities of density peaks.

According to linear theory of gravitational instability in a dust universe (Peebles 1980), the peculiar velocity field of mass grows as

$$v \propto a\dot{D} = \dot{a}D \frac{d \ln D}{d \ln a}$$

$$= \dot{a}D(a) \left[ \frac{5\Omega_0}{2D(a)X(a)^2} + \frac{\Lambda_0 a^2 - \Omega_0/2a}{X(a)^2} - 1 \right], \quad (1)$$

where

$$X(a) = \frac{\dot{a}}{H_0} = \left[ \frac{\Omega_0}{a} + (1 - \Omega_0 - \Lambda_0) + \Lambda_0 a^2 \right]^{\frac{1}{2}}. \quad (2)$$

The linear growth factor  $D(a)$  is given by

$$D(a) = \frac{5\Omega_0}{2} \frac{X(a)}{a} \int_0^a \frac{da'}{X(a')^3}. \quad (3)$$

Note that the frequently used approximation  $f(a) = d \ln D / d \ln a \simeq \Omega^{0.6}$  underestimates the growth rate by  $\sim 5$  percent in the flat  $\Omega_0 = 0.3$  cosmology that we consider here. Thus, we will not adopt the approximation but we will use the numerical integration throughout the present paper.

We assume that the primordial (linear) density fluctuations obey the Gaussian statistics. Then the peculiar velocity field is isotropic and Gaussian, and its three-dimensional dispersion smoothed over a smoothing scale of  $R$  is given by

$$\sigma_v(R, a) = \dot{a}f(a)\sigma_{-1}(R, a). \quad (4)$$

Following Bardeen et al. (1986),  $\sigma_j$  is defined for any integer  $j$  as

$$\sigma_j^2(R) = \frac{1}{2\pi^2} \int dk k^{2+2j} P(k) W^2(kR), \quad (5)$$

where  $W(x)$  is the Fourier transform of the smoothing window, and  $P(k)$  is the linear matter power spectrum. Throughout this paper, we use the real space top-hat window function which corresponds to  $W(x) = (3/x^3)[\sin(x) - x \cos(x)]$ . We adopt the fitting function of a cold dark matter (CDM) power spectrum given by Bardeen et al. (1986), who show that the rms peculiar velocity at the peaks of the smoothed density field differs systematically from  $\sigma_v$  by

$$\sigma_p(R) = \sigma_v(R) \sqrt{1 - \sigma_0^4 / \sigma_1^2 \sigma_{-1}^2}. \quad (6)$$

Note that this expression does not depend on the height of peaks.

The conventional assumptions in modeling the peculiar velocities of halos are as follows. (i) The velocities of halos are identical to those of peaks (equation 6). The smoothing scale is chosen such that the filtered mass is equal to that of the halo considered, i.e.,  $M = 4\pi\bar{\rho}R^3/3$  in the case of the real space top-hat window function. (ii) The halo velocities evolve according to linear theory (equation 1). However, the prediction based on these assumptions seems to underestimate the rms peculiar velocities of halos (Colberg et al. 2000).

## 3 N-BODY SIMULATION

In constructing an improved model of the peculiar velocity of halos, we first use  $N$ -body simulations of a  $\Lambda$ CDM cosmology ( $\Omega_0 = 0.3$ ,  $\Lambda_0 = 0.7$ ,  $h = 0.7$ , and  $\sigma_8 = 1.0$ ). The details of the  $N$ -body simulations are described in Jing & Suto (1998); see also Kayo et al. (2001). Briefly, the simulations employ  $256^3$  CDM particles in a cubic box of  $300 h^{-1}$  Mpc on a side. The simulations are performed using a  $P^3M$  code with the gravitational softening length of  $\epsilon \sim 120 h^{-1}$  kpc. The initial matter power spectrum is computed using the CDM fitting function given by Bardeen et

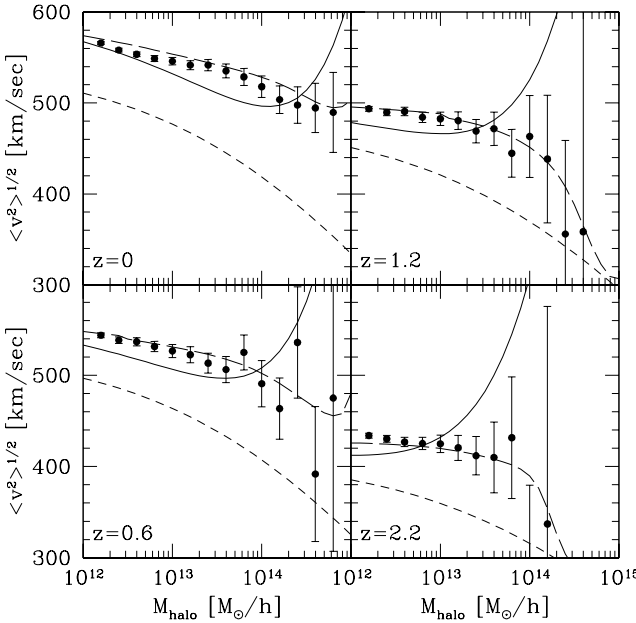


**Figure 1.** Halo velocity dispersions as a function of halo mass at different redshifts as indicated in each panel. Filled circles are measurements from  $N$ -body simulations. The long-dashed lines represent the phenomenological model, equation (8) adopting the conditional mass function via equation (9), while solid lines are for the model with the approximation equation (10). The dashed lines show the linear theory prediction for peaks (equation 6).

al. (1986). We have three realizations which differ only in the phases of the initial density fluctuations. The particle mass ( $m_{\text{part}} = 1.34 \times 10^{11} h^{-1} M_{\odot}$ ) of the simulations is sufficiently small to guarantee that there are practically no discreteness effects on dark matter clustering on scales down to the softening length in the redshift range of interest for our purposes (Hamana, Yoshida & Suto 2002).

We identify dark matter halos using the standard friends-of-friends algorithm with a linking parameter of  $b = 0.164$  (in units of the mean particle separation). We set the minimum mass of the halos as  $1.34 \times 10^{12} h^{-1} M_{\odot}$ , which corresponds to the mass of 10 simulation particles. We define the peculiar velocity of each halo to be the center-of-mass peculiar velocity of member particles.

The smoothed mass density fields are computed on  $64^3$  regular grids in the simulation box using the top-hat window function. For each halo, the smoothed mass density of the nearest grid is assigned as its local background density.

Fig. 1 shows the rms peculiar velocities of halos in the  $N$ -body simulation (filled circles) together with the linear theory prediction of peaks, (equation 6; dashed curves) as well as our predictions described in the next section (solid lines and long-dashed lines). Note that, in order to account for the finite size of the simulation box ( $L_{\text{box}} = 300 h^{-1} \text{Mpc}$ ), we set a lower limit of the integration in equation (5) by  $k_{\text{min}} = 2\pi/L_{\text{box}}$ . This large-scale cut-off reduces  $\sigma_p$  by a fractional amount of about 8 percent, and is applied to all model predictions in this paper. The plot confirms the previous finding that the linear theory predictions underestimate the rms peculiar velocities by about 10–40 percent for cases  $0 < z < 2.2$  in a  $\Lambda$ CDM cosmology. In addition, it is seen from this Figure that the linear theory predictions have a

slightly steeper slope than that of  $N$ -body simulations, especially for the case of  $z = 0$ . This discrepancy may be explained by the following: (i) massive halos tend to be formed in denser regions as a result of the biasing mechanism, and (ii) halos in denser regions move faster than those in less dense regions, as will be proved in the next section (Fig. 2 and 4). As a consequence, on average, deviations from linear theory appear larger for massive halos, and thus the slope of  $N$ -body data becomes flatter.

#### 4 MODEL

In this section, we describe our model of the rms peculiar velocity of halos. We basically follow the framework developed by Sheth & Diaferio (2001); see also Diaferio & Geller (1996) and Sheth (1996). They originally developed the model for the distribution function of peculiar velocities of dark matter particles and halos, but their framework can be straightforwardly applied to the model for the rms of halo peculiar velocities.

Sheth & Diaferio (2001) pointed out that the evolution of the halo peculiar velocity depends on the local matter density (defined with an appropriate smoothing length which we discuss later). We thus first construct a model for the dependence of the halo peculiar velocity dispersion,  $\sigma_{\text{halo}}^2(M, \delta)$ , on the local background density  $\delta$ . Following Sheth & Diaferio (2001), we consider a parametric model

$$\sigma_{\text{halo}}^2(M, \delta) = [1 + \delta(R_{\text{local}})]^{2\mu(R_{\text{local}})} \sigma_p^2(M), \quad (7)$$

where  $R_{\text{local}}$  is the smoothing scale with which the local background density  $\delta$  is defined. The key question is how to define the *appropriate* smoothing length-scale. Evidently,  $R_{\text{local}}$  should enclose the gravitational coherence scale which is responsible for the local deviation of the peculiar motion of a halo from its global value (for instance, given by linear theory). Thus, the size of halo (e.g., the virial radius) sets a lower limit for  $R_{\text{local}}$ . On the other hand, choosing values for  $R_{\text{local}}$  that are too large would result in an excessively smoothed density field, and local density fluctuations, by which the deviation from the global value is induced, are smoothed out. We may, thus, expect that  $R_{\text{local}}$  is in the range between the linear scale (such that  $\sigma_0(R) < 1$ ) and the non-linear scale ( $\sigma_0(R) > 1$ ). Concerning the power-law index  $\mu$ , the linear theory relation,  $f \propto \Omega^{0.6}$ , suggests  $\mu \simeq 0.6$  (Sheth & Diaferio 2001). Note, however, that  $\mu$  depends on  $R_{\text{local}}$  on which the local density is defined (a larger  $\mu$  for a larger smoothing length, because the range of  $\delta$  becomes narrower), thus  $\mu$  does not need to be very close  $\mu \simeq 0.6$ , but it is expected that with an appropriate choice of the smoothing length-scale,  $\mu$  would be close to 0.6.

To proceed further, we adopt an ansatz that  $R_{\text{local}}$  is given by a relation  $\sigma_0(R_{\text{local}}) = \sigma_{\text{local}}$ , and we determine the model parameter  $\sigma_{\text{local}}$  empirically using  $N$ -body simulations. As expected from the discussion above, a suitable choice of  $\sigma_{\text{local}}$  would be within a range  $0.1 < \sigma_{\text{local}} < 1$ . We find that choosing  $\mu = 0.6$  (constant) with  $R_{\text{local}}$  given by  $\sigma_{\text{local}} = 0.5(1+z)^{-0.5}$  (through  $\sigma_0(R_{\text{local}}) = \sigma_{\text{local}}$ ) provides reasonable fits to the results of the  $N$ -body simulations as shown in Fig. 2. For this choice,  $R_{\text{local}} \simeq 18$  and  $16 h^{-1} \text{Mpc}$  for  $z=0$  and 0.8, respectively. The value of  $\mu = 0.6$  is consistent with one suggested in linear theory ( $\mu \simeq 0.6$ ). Thus,

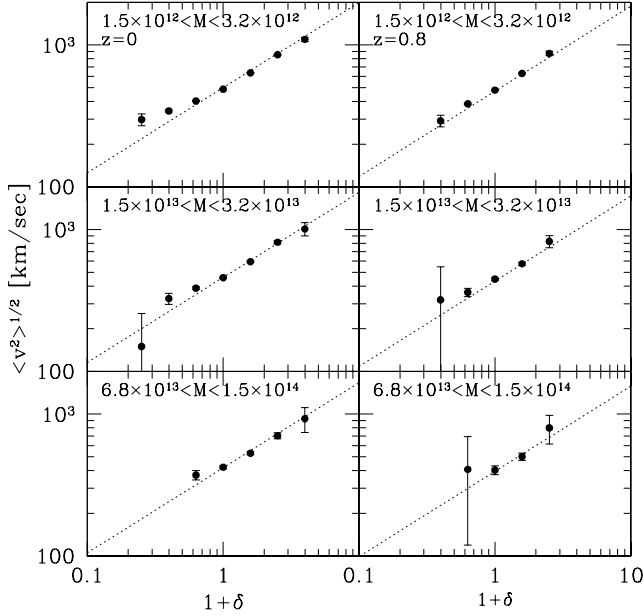


**Figure 2.** Halo peculiar velocity dispersions as a function of the local background density for limited mass ranges. Halo mass ranges (in units of  $h^{-1} M_{\odot}$ ) are denoted in each plot. Dotted lines represent the model equation (7) with  $\mu = 0.6$  and filled circles show measurements from our  $N$ -body simulations. The smoothed local density fields are computed from the  $N$ -body particle distributions using the top-hat window function with a smoothing scale of  $20h^{-1}\text{Mpc}$ .

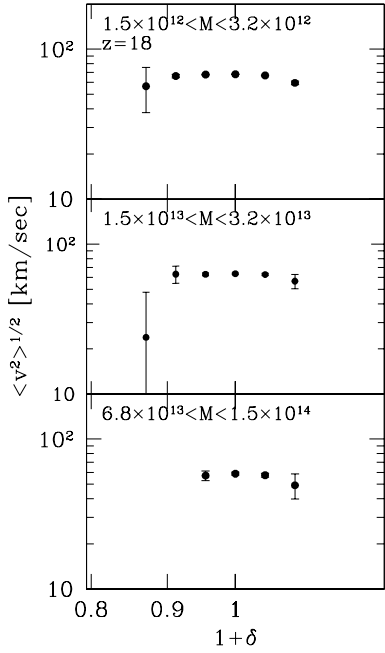


**Figure 3.** Same as Fig. 2 but for halo progenitors at the initial redshift of the  $N$ -body simulation ( $z = 18$ ). We mark the member particles of a halo identified at  $z = 0$ , and then compute the position and velocity of the halo progenitor from the center-of-mass position and velocity of the marked particles at  $z = 18$ . The top-hat smoothing scales for computing the local density are taken to be  $20h^{-1}\text{Mpc}$ .

while the choice of the smoothing length may still be arbitrary, we decide to use the above sets of parameters for definiteness.

Fig. 3 shows the peculiar velocity dispersion of halo progenitors as a function of the local density at the initial redshift of the  $N$ -body simulation  $z = 18$ . We mark the member particles of a halo identified at  $z = 0$ , and then compute the position and velocity of the halo progenitor from the center-of-mass position and velocity of the marked particles at  $z = 18$ . Fig. 3 clearly indicates that there is no clear correlation between the peculiar velocity and the local density at the initial epoch. Together with Fig. 2, this strongly supports the idea that most of the halo peculiar velocity is acquired through the subsequent evolution of the nearby density field. A closer look at Fig. 3 reveals that the initial peculiar velocity dispersions decline very slightly at both the lowest and highest bins. An interpretation of this is that, at the initial epoch, the halo progenitors locate close to positive (negative) density peaks tend to have relatively higher (lower) local densities. At the same time, a potential gradient at positions close to the density peaks tends to be small, and thus the progenitors at such regions move slower than others. As a result, the highest and lowest density bins have a slightly lower peculiar velocity than other bins.

As shown by Sheth & Diaferio (2001), if the range of halo masses and local background density is sufficiently small, the PDF of halo peculiar velocities is well approximated by a Maxwellian distribution, i.e., the PDF of one-dimensional velocity is a Gaussian. We denote by  $p(M|\delta)$  the probability of finding a halo with mass  $M$  at a region where the background density is  $\delta$ . Then the peculiar velocity dispersion of halos with mass  $M$  is given by summing up the dispersion  $\sigma_{\text{halo}}^2(M, \delta)$  weighted over the probability of finding halos in regions of  $\delta$ :

$$\sigma_{\text{halo}}^2(M) = \frac{\int d\delta p(M|\delta) \sigma_{\text{halo}}^2(M, \delta)}{\int d\delta p(M|\delta)}. \quad (8)$$

Note that this expression is valid only if the background density is defined appropriately (i.e., with the smoothing scale  $R_{\text{local}}$  defined above). The expression for  $p(M|\delta)$  is obtained as follows.

It is well established that dark matter halos are biased tracers of the underlying dark matter distribution. In this picture, it is useful to write the conditional probability as

$$p(M|\delta) = \frac{n(M|\delta)}{n(M)} p_{dm}(\delta), \quad (9)$$

where  $n(M)$  and  $n(M|\delta)$  denote the halo mass function and the *conditional* mass function in regions with the local background density  $\delta$ , respectively, and  $p_{dm}(\delta)$  is the PDF of the dark matter density field. To evaluate the first term of the right hand side of equation (9), i.e. the excess number density of halos, we adopt two approaches. The first is to directly use the mass functions derived from the extended model of Press-Schechter (1974); see, for example, Bond et al. (1991). Lacey & Cole (1991) and Mo & White (1996). In practice, we adopt the conditional mass function given by Sheth & Tormen (2002) that even takes into account the effect of the ellipsoidal collapse. The other approach is to use a simple approximation,  $n(M|\delta) \simeq [1 + b(M)\delta]n(M)$ . Note that this approximation is valid only if the smoothing scale defining the local density is much larger than the halo size, or equiv-

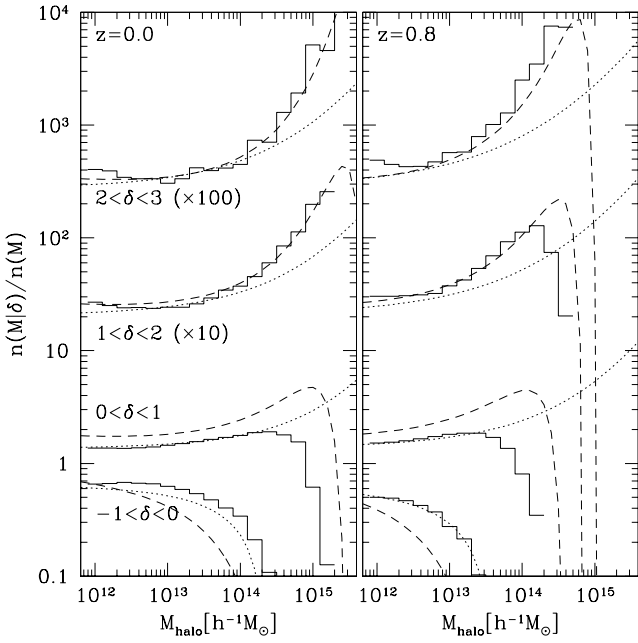


**Figure 4.** Conditional mass functions normalized by the unconditional mass function for ranges of the local background density, from lower to upper,  $-1 < \delta < 0$ ,  $0 < \delta < 1$ ,  $1 < \delta < 2$  and  $2 < \delta < 3$ . Dashed curves show the conditional mass function by Sheth & Tormen (2002), dotted curves show the approximation  $n(M|\delta) \simeq [1 + b(M)\delta]n(M)$  with the unconditional mass function and halo bias model by Sheth & Tormen (1999), and the solid histograms are for  $N$ -body data. The top two cases are offset upward by a factor of 10 and 100. The smoothing scales for computing the local density are  $R_{\text{local}} = 20$  and  $10h^{-1}\text{Mpc}$  for  $z = 0$  (left panel), and 0.8 (right panel), respectively.

alently if the total mass enclosed within the smoothing scale is much larger than the halo mass. Adopting this, equation (9) reduces to

$$p(M|\delta) = [1 + b(M)\delta]p_{dm}(\delta). \quad (10)$$

Mo & White (1996) developed a Lagrangian halo bias model based on the extended Press-Schechter model. Jing (1998) and Sheth & Tormen (1999) discussed the correction for the mass dependence of the halo bias and proposed modified fitting functions that give better fits to numerical simulation results. In what follows, we use the linear bias model of Sheth & Tormen (1999). Although the former approach may lead to a better model than the latter, we examine the latter approximation to see if the simple approach could provide an acceptable model. Fig. 4 compares the above two theoretical predictions (dashed and dotted lines) for  $n(M|\delta)/n(M)$  with the  $N$ -body data (solid histograms) for ranges of the local background density. The simple approximation  $n(M|\delta) \simeq [1 + b(M)\delta]n(M)$  turns out to provide a good fit to the  $N$ -body data for smaller mass ranges  $M_{\text{halo}} < 10^{13\sim 14}h^{-1}M_{\odot}$ , but underestimates the conditional probability for larger mass ranges. The conditional mass function by Sheth & Tormen (2002) gives good fits for high local densities ( $\delta > 1$ , upper two cases in the plots), while fits become degraded for low densities ( $\delta < 1$ , lower two cases in the plots). Importantly, it reproduces the cut-off in the conditional mass function at a large mass nicely in

marked contrast to the approximation which does not have the cut-off.

The dark matter PDF is known to be well fitted to the log-normal distribution (e.g., Coles & Jones 1991; Kofman et al. 1994; Kayo, Taruya & Suto 2001; see also Taruya, Hamana & Kayo 2003 for a possible explanation of the origin of the log-normal PDF)

$$p_{ln}(\delta) = \frac{1}{(2\pi\sigma_1^2)^{1/2}} \exp \left\{ -\frac{[\ln(1 + \delta) + \sigma_1^2/2]^2}{2\sigma_1^2} \right\} \frac{1}{1 + \delta} \quad (11)$$

where  $\sigma_1$  is related to the variance of the nonlinear density field by

$$\sigma_1^2(R) = \ln[1 + \sigma_{nl}^2(R)], \quad (12)$$

with

$$\sigma_{nl}^2(R) = \frac{1}{2\pi^2} \int dk k^2 P_{nl}(k) W^2(kR). \quad (13)$$

In the above expression,  $P_{nl}(k)$  denotes the nonlinear matter power spectrum for which we compute using the fitting function of Peacock & Dodds (1996).

## 5 RESULTS

Fig. 1 compares our model predictions with  $N$ -body simulations (filled circles); long-dashed curves correspond to equation (9) with the conditional mass function by Sheth & Tormen (2002), while solid curves correspond to the approximation equation (10). It is clear that our models (especially the former one) substantially improve the accuracy of the prediction compared with that of linear theory (dotted lines) except for a very high mass range of  $M > 10^{14}h^{-1}M_{\odot}$ . However, the predictions of the model adopting the approximation equation (10) rise very rapidly at a high mass range of  $M > 10^{14}h^{-1}M_{\odot}$  and significantly deviate from the simulation results. This is explained as follows: As shown in Fig. 4, the conditional mass function computed from  $N$ -body simulation declines at a high mass range. However, the approximation equation (10) does not reproduce this feature but keeps on rising toward a large halo mass. Consequently, the approximated model over-estimates the contribution from moderately over density regions. Here, it must be noted that with our choice of the smoothing scale ( $R_{\text{local}} = 18, 15$  and  $13h^{-1}\text{Mpc}$  for  $z = 1, 2$  and 3, respectively), the most of the matter in the universe is in regions where the local density contrast being  $-1 < \delta < 1$ . Therefore, a discrepancy in the conditional mass function at a high density range of  $\delta > 1$  between the model and the simulation does not have a large influence on the model prediction. Adopting the conditional mass function proposed by Sheth & Tormen (2002), which reasonably reproduces the decline as shown in Fig. 4, improves the accuracy of the prediction very well. In particular, this model predicts a flatter slope than that of the linear theory prediction, and it is very close to the simulation results. We, however, note that the model prediction adopting Sheth & Tormen conditional mass function rises at very large mass scales ( $M > 10^{15}$ ) and deviates from the simulation. The reason of this is that the conditional mass function becomes less accurate at such mass range. Because at that mass range, the number density of halos is too small

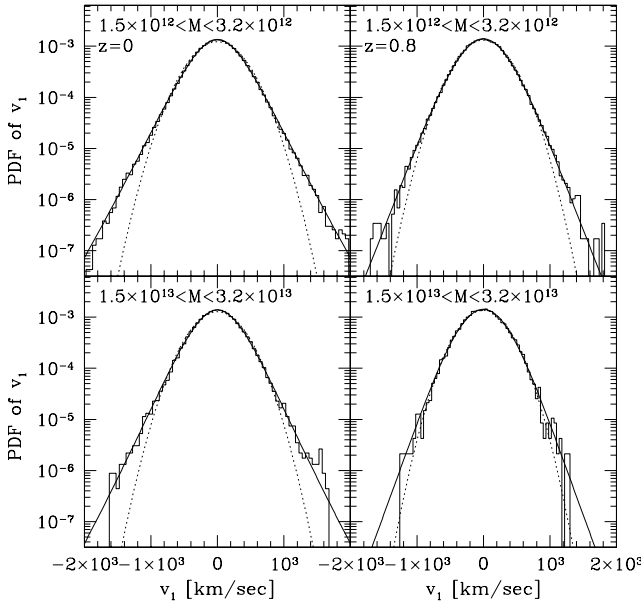


**Figure 5.** PDFs of one-dimensional halo velocity  $v_1$  at  $z = 0$  (left panels) and  $z = 0.8$  (right panels) and for limited mass ranges (denoted in each plot). Histograms show the measurement from the  $N$ -body simulations. Solid curves show our model prediction, while dotted curves represent the Gaussian distribution with  $\sigma$  computed from the  $N$ -body simulation.

to have a meaningful statistic, this disagreement is not serious.

Although there is still room for improvement in the model, our model adopting the conditional mass function of Sheth & Tormen (2002), provides a good fit to the  $N$ -body data over a wide range of the halo mass. To improve the model prediction, it may be necessary to adopt a further developed conditional mass function. Developing an accurate conditional mass function is beyond the scope of the present paper, and hence we do not attempt this here. In the following discussions, we adopt the model adopting Sheth & Tormen conditional mass function.

As Sheth & Diaferio (2001) originally showed, the model presented in this paper is applied to model the PDF of halo peculiar velocities

$$P(v|M) = \frac{\int d\delta p(M|\delta)P(v|M,\delta)}{\int d\delta p(M|\delta)}, \quad (14)$$

where  $P(v|M)$  is the PDF of peculiar velocities of halos with mass  $M$ , and  $P(v|M,\delta)$  is the PDF for halos at regions with the local background density  $\delta$ . The PDF of one-dimensional peculiar velocities (which we denote by  $v_1$ ),  $P(v_1|M,\delta)$ , is well approximated by the Gaussian distribution (Sheth & Diaferio 2001). We compute  $\sigma$  of the Gaussian PDF using equation (7) with a reasonable isotropic assumption  $\langle v_1^2 \rangle = \langle v^2 \rangle / 3$ . The results are plotted in Fig. 5 (solid lines), and are compared with  $N$ -body simulations (histograms) and Gaussian PDF (dotted lines). As Fig. 5 clearly shows, our model agrees with the  $N$ -body simulation very well. Also it is seen from the Figure that the PDF of one-dimensional peculiar velocity consists of two parts; a Gaussian core and an exponential tail. The exponential tail arises from the sum of Gaussian distributions with differ-

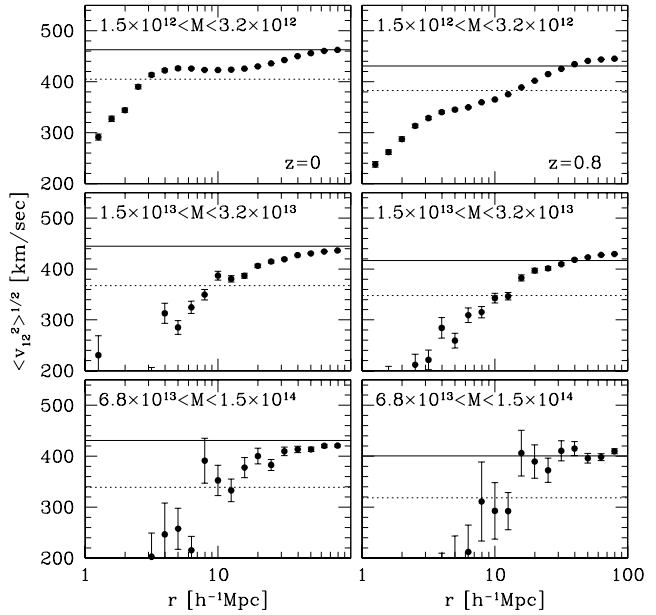


**Figure 6.** Pairwise velocity dispersion of halos as a function of the separation for limited mass ranges (denoted in each plot). Filled circles indicate the  $N$ -body results. Dotted lines represent the linear theory prediction for peaks neglecting velocity correlation,  $\langle v_{12}^2 \rangle^{1/2} = \sqrt{2/3}\sigma_p$ , while solid lines show our model prediction  $\langle v_{12}^2 \rangle^{1/2} = \sqrt{2/3}\sigma_{\text{halo}}$ .

ent dispersions (Sheth & Diaferio 2001; Kuwabara, Taruya & Suto 2002). Our model nicely reproduces the deviation from the Gaussian distribution at large peculiar velocities and agrees with the simulation very well.

The model presented in this paper can be also applied to the pairwise velocity dispersion of halos at large distances. The model of the pairwise velocity dispersion plays an important role in computing the redshift distortion of the two-point correlation function of halos. Because any velocity correlation between halos with large separations of  $r > 20h^{-1}\text{Mpc}$  may be safely ignored, the halo pairwise velocity dispersion is given by  $\langle v_{12}^2 \rangle = 2/3\langle v^2 \rangle$ , where  $v_{12}$  denotes the pairwise velocity of a pair of halos. Often  $\sigma_p^2$  (equation 6) is used to compute  $\langle v^2 \rangle$  (e.g., Hamana et al. 2001); see Sheth et al. 2001a,b for an alternative approach. However, as shown in the previous sections, the linear theory prediction underestimates the halo velocity and our model provides better fits to  $N$ -body data. We may, therefore, expect that our model improves predictions of the pairwise velocity dispersion. Fig. 6 compares the model prediction for the pairwise velocity dispersion (solid lines) with the result of our  $N$ -body simulation (filled circles). We also plot the linear theory prediction for peaks (dotted lines). As Fig. 6 clearly shows, our model indeed improves the accuracy of prediction at  $r > 20h^{-1}\text{Mpc}$ .

## 6 SUMMARY AND DISCUSSIONS

We present a model of peculiar velocities of dark matter halos which describes various statistical properties well and significantly improves the accuracy of the simple linear theory predictions, including the halo rms velocity dispersion,

PDF, and the pairwise velocity dispersion at large separations. The model predictions, however, becomes less accurate for very large halo masses ( $M > 10^{15} h^{-1} M_{\odot}$ ). This is mainly due to the limitation of the adopted conditional halo mass function, and may be reconciled by using an improved model. Note that this shortcoming hardly causes any practical problem, because the number density of such very massive halos is too small to have a meaningful statistic.

The model presented in this paper is characterized by a single free parameter,  $\mu(R_{\text{local}})$ , that we determine in an empirical manner. To do this, we need the appropriate smoothing scale for the current purpose. We make an anzats that  $R_{\text{local}}$  is in the range between the linear and the non-linear scale and it should be given by the relation  $\sigma_0(R_{\text{local}}) = \sigma_{\text{local}}$  for some value in a range  $0.1 < \sigma_{\text{local}} < 1$ . This turns out to be reasonably successful, and we have found that a choice of  $\mu = 0.6$  with  $\sigma_{\text{local}} = 0.5(1+z)^{-0.5}$  works well for all redshifts we consider in this paper ( $z < 2.2$ ). This choice gives the smoothing scales of  $R_{\text{local}} = 18, 15, 11, 8.5$  and  $5.6 h^{-1} \text{Mpc}$  for  $z = 0, 1, 3, 5$  and  $10$ , respectively. However, we calibrated the model with  $N$ -body data at  $0 < z < 2.2$  only, thus the validity of this procedure is questionable for very higher redshifts (although in practice velocities of halos at very high redshifts are not observable currently). A more sophisticated approach to the choice of the smoothing scale is needed for a further improvement of the model. This may be closely connected to an understanding of the role of the local environment in the structure formation, and is a subject of work in progress.

## ACKNOWLEDGMENTS

We thank the referee, Ravi Sheth, for detailed and constructive comments on the earlier manuscript which significantly improves various aspects of the paper. We thank Joerg M. Colberg for alerting us to the mistake in the original version of this paper. T.H. acknowledges supports from Japan Society for Promotion of Science (JSPS) Research Fellowships. Y.I.P. is supported in part by NKBRSF (G19990754) and by NSFC (No. 10125314). This work was supported in part by the Grant-in-Aid for Scientific Research of JSPS (12640231). Numerical computations presented in this paper were carried out at the Astronomical Data Analysis Center of the National Astronomical Observatory, Japan (project ID: mys02a).

## REFERENCES

Aghanim N., Górski K. M. & Puget J.-L., 2001, 374, 1  
 Bahcall N.A., Gramann M., Cen R. 1994, ApJ, 436, 23  
 Bardeen J. M., Bond J. R., Kaiser N., Szalay A. S. 1986, ApJ, 304, 15  
 Bond J. R., Cole S., Efstathiou G., Kaiser N., 1991, ApJ, 379, 440  
 Borgani S., da Costa L. N., Freudling W., Giovanelli R., Haynes M. P., Salzer, J., Wegner, G. 1997, ApJ, 482, L121  
 Borgani S., Bernardi M., da Costa L. N., Wegner G., Alonso M. V., Willmer C. N. A., Pellegrini P. S., Maia M. A. G., 2000, ApJ, 537, L1  
 Colberg J. M., White S. D. M., MacFarland T. J., Jenkins A., Pearce F. R., Frenk, C. S., Thomas P. A., Couchman H. M. P., 2000, MNRAS, 313, 229  
 Cole S., 1997, MNRAS, 386, 38  
 Coles P., Jones B. 1991, MNRAS, 248, 1  
 Colless M., Saglia R. P., Burstein D., Davies R. L., McManan R. K., Wegner G., 2001, MNRAS, 321, 277  
 Croft R. A. C., Efstathiou G., 1994, MNRAS, 268, L23  
 Dale D. A., Giovanelli R., Haynes M. P., Campusano L. E., Hardy E. 1999, AJ, 118, 1489  
 Diaferio A., Geller M., 1996, ApJ, 19  
 Haehnelt M. G., Tegmark M., 1996, MNRAS, 279, 545  
 Hamana T., Yoshida N., Suto Y., 2002, ApJ, 568, 455  
 Hamana T., Yoshida N., Suto Y., Evrard A. E., 2001, ApJ, 561, L143  
 Hudson M. J., Smith R. J., Lucey J. R., Schlegel D. J., Davies R. L., 1999, ApJ, 512, L79  
 Jenkins A., Frenk C.S., White S.D.M., Colberg J.M., Cole S., Evrard A.E., Couchman H.M.P., Yoshida N., 2001, MNRAS, 321, 372  
 Jing Y. P., 1998, ApJ, 503, L9  
 Jing Y. P., 2000, ApJ, 535, 30  
 Jing Y. P., Suto Y., 1998, ApJ, 494, L5  
 Jing Y. P., Suto Y., 2000, ApJ, 529, L69  
 Kashlinsky A., Atrio-Barandela F., 2000, ApJ, 536, L67  
 Kayo I., Taruya A., Suto Y., 2001, ApJ, 561, 22  
 Kepner J. V., Summers F. J., Strauss M. A., 1997, New Astronomy, 2, 165  
 Kofman L., Bertschinger E., Gelb J.M. Nusser A., Dekel A., 1994, ApJ, 420, 44  
 Kuwabara T., Taruya A., Suto, Y. 2002, PASJ, 54, 503  
 Lacey C., Cole S. 1993, MNRAS, 262, 627  
 Lauer T. R., Postman M. 1994, ApJ, 425, 418  
 Mo H. J., White S. D.M. 1996, MNRAS, 282, 347  
 Moscardini L., Branchini E., Brunozzi P. T., Borgani S., Plionis M., Coles P. 1996, MNRAS, 282, 384  
 Peacock J.A., Dodds S.J., 1996, MNRAS, 280, L19  
 Peebles, P. J. E., 1980, The Large-Scale Structure of the Universe Princeton Univ. Press, Princeton, NJ  
 Press W. H., Schechter P., 1974, ApJ, 187, 425  
 Rephaeli Y., Lahav O. 1991, ApJ, 372, 21  
 Sheth R. K., 1996, MNRAS, 279, 1310  
 Sheth R. K., Diaferio A., 2001, MNRAS, 322, 901  
 Sheth R. K., Diaferio A., Hui L., Scoccimarro R., 2001a, MNRAS, 326, 463  
 Sheth R. K., Hui L., Diaferio A., Scoccimarro, R., 2001b, MNRAS, 325, 1288  
 Sheth R. K., Tormen G., 1999, MNRAS, 308, 119  
 Sheth R. K., Tormen G., 2002, MNRAS, 329, 61  
 Suhhonenko I., Gramann M., 1999, MNRAS, 303, 77  
 Sunyaev R. A., Zel'dovich Y. B., 1980, MNRAS, 190, 413  
 Taruya A., Hamana T., I. Kayo, 2003, MNRAS, 339, 495  
 Taruya A., Suto Y. 2000, ApJ, 542, 559  
 Tormen G., Bertschinger, E., 1996, AJ, 472, 14  
 Yoshida N., Sheth R. K., Diaferio A., 2001, MNRAS, 328, 669